Stochastic Environmental Research and Risk Assessment (2024) 38:1669–1684
https://doi.org/10.1007/s00477-023-02654-3

ORIGINAL PAPER

Sensitivity analysis in the wavelet domain: a comparison study

Gabriele Chiogna[1,2] · Giorgia Marcolini[1,3] · Michael Engel[1] · Barbara Wohlmuth[3]

Accepted: 29 December 2023 / Published online: 12 January 2024

Abstract
Sensitivity analysis plays a pivotal role for the development and calibration of hydrological models, since they are often affected by equifinality. Despite a lot of effort has been placed for the development of effective sensitivity analysis methods, hydrological models remain over parametrized. We take advantage of the evidence that hydrological processes can be described as the superposition of effects occurring at different temporal scales (e.g., seasonal precipitation patterns, seasonal and daily snow and glacier melt, seasonal, daily and sub-daily water management operations) to develop a new framework to perform sensitivity analysis. We apply discrete and continuous wavelet transforms to disentangle hydrological signals occurring at different temporal scales and we take advantage of the different information stored at different temporal scales of the wavelet spectrum to perform a scale-dependent sensitivity analysis. This approach aims to increase the number of identifiable model parameters in comparison to standard sensitivity analysis performed in the time domain. As an exemplary problem, we apply the methodology to synthetic data describing surface water-groundwater interaction in rivers affected by hydropeaking (i.e., sudden fluctuations in the river stage due to hydropower production). The method could be applied also to other models displaying the superposition of processes with different intensities at different temporal scales such as ocean tide propagation in aquifers as well as snow and glacier melt models. The results indicate that considering multiple temporal scales allows us to increase the number of parameters that can be identified and hence calibrated with only a little increase in the computational effort.

Keywords Sensitivity analysis · Sobol index · Wavelet · Periodogram efficiency criterion · Hydropeaking · Surface water-groundwater interaction

1 Introduction

Sensitivity analysis is an important step in the development of reliable hydrological models to interpret, reproduce and forecast surface and subsurface hydrological processes (Brunetti et al. 2018; Ciriello et al. 2013; Dell'Oca et al. 2017; Pianosi et al. 2016). When sensitivity analysis is performed in the context of model calibration (Siena and Riva 2020; Yang et al. 2017), assuming that we have a perfect hydrological model, we could hope that all model parameters can be constrained by using the available observations and hence all parameters are sensitive (Wagener and Pianosi 2019). However, this is generally not the case (Beven 2006; Schöniger et al. 2014). In fact, hydrological models are often over parametrized (Kirchner 2006; Samaniego et al. 2010; Seibert et al. 2019), they require parameters that cannot be accurately determined by performing inverse modeling (Guse et al. 2020) or changes in the value of some model parameters have only a limited effect on the quantity of interest that is considered for model calibration, such as river discharge or hydraulic head in an aquifer (Borgonovo et al. 2017). Due to equifinality (i.e., the existence of multiple optimal parameter sets that reproduce the observed values), the identification of model parameters is a challenging task and sensitivity analysis can support in the assessment of which model parameters can be effectively constrained considering the available data.. Moreover, hydrological processes display a complex temporal dynamic, which may lead to the identification of time-dependent sensitive parameters.

✉ Gabriele Chiogna
gabriele.chiogna@tum.de

[1] School of Engineering and Design, Technical University of Munich, Munich, Germany

[2] Institute of Geography, University of Innsbruck, Innsbruck, Austria

[3] Department of Numerical Mathematics, Technical University of Munich, Garching, Germany

Song et al. (2015) include the topic of time-dependent sensitivity analysis in their review paper. The aim of time-dependent sensitivity analysis is in general to assess the dynamics and the interplay among model parameters and processes under specific hydrological conditions or time windows (Bittner et al. 2021b; Herman et al. 2013; Reusser et al. 2011). Time-dependent sensitivity analysis aims at increasing parameter identifiability and at recognizing the different uncertainty sources in time, leading therefore to more reliable hydrological models (Pianosi and Wagener, 2016). A critical aspect of this approach relies in the choice of the events and their representativeness, in particular in case of hydrological problems characterized by a wide range of variability (Meles et al. 2021).

An alternative approach to the definition of time-dependent sensitivities is to perform a sensitivity analysis for the temporal scales (levels) in which a signal can be subdivided after wavelet decomposition (Bittner et al. 2021a, 2020). Wavelet transforms are calculated by passing a signal through a series of filters (Torrence and Compo 1998). After the application of each filter, the signal is decomposed into low and high frequencies. Several hydrological studies took advantage of wavelet decomposition to detect changes in the frequency components of the signal characterized by some intermittency and to determine the dominant temporal scales of variability of a time series (Ciria et al. 2019; Rossi et al. 2009; Wang et al. 2014; Zolezzi et al. 2009). Therefore, wavelet transform showed that different hydrological processes contribute to different temporal scales of the same hydrological observations. Consequently, specialized models that require specific parameters and that affect different temporal scales are used to represent different hydrological processes characterized by specific temporal variabilities. Moreover, wavelet transform was applied for the assessment of model performance (Chiogna et al. 2018; Rathinasamy et al. 2014) and model calibration (Duran et al. 2020; Schaefli and Zehe 2009). In the context of sensitivity analysis, wavelet decomposition has been applied by Bittner et al. (2021a) coupling it with the active subspace model reduction technique and they proved that different parameters are sensitive on different temporal scales. Xiao et al. (2018) introduced a method to compute sensitivity indices for the model parameters based on the wavelet decomposition of the model output and then merging the information obtained for the different scales.

In this study, we compare four different approaches to detect sensitive parameters using global sensitivity analysis. One method is based on the computation of the Sobol index (Saltelli et al. 2010) in the time domain, while three new approaches compute the Sobol index in the wavelet frequency domain. The first approach to detect sensitive parameters in the wavelet domain is based on the discrete wavelet transform of the model output and on the computation of the Sobol indices (Smith 2013) for each temporal scale separately. The second approach considers as objective function for the computation of the Sobol indices the wavelet periodogram efficiency criterion introduced by Schaefli and Zehe, (2009). The last approach considers an objective function which combines the wavelet periodogram efficiency criterion and the mean absolute error in the time domain. The use of discrete and continuous wavelet transform in the sensitivity analysis has the goal to isolate the effects of parameters contributing only to specific temporal scales which may or may not be dominant in the whole signal.

We test and compare the four methods to the problem of surface water-groundwater interaction under transient conditions proposed by Hucks Sawyer et al. (2009), using synthetic data. In particular, the analytical solution describes the aquifer response to a river affected by hydropeaking, i.e. sudden fluctuations of the river stage caused by hydropower production (Hauer et al. 2017). Such fluctuations, caused by the energy market variability, occur at multiple temporal scales (e.g., sub-daily, daily and weekly) and have important implications for the riverine ecosystem (Bruder et al. 2016) as well as for energy and mass transfer in aquifers (Basilio Hazas et al. 2022; Ferencz et al. 2019; Ziliotto et al. 2021). The variability in the amplitude and frequency of the hydropeaking wave is an information that hydropower companies are not obliged to share and adds on the typical uncertainty parameters typically encountered in hydrogeological studies, such as hydraulic conductivity, specific yield and aquifer thickness. Therefore, it is relevant to assess the share of uncertainty introduced in our model prediction by anthropogenic operations and by natural geological properties of the aquifer. Similar problems displaying the superposition of processes occurring with different intensities at different temporal scales are not rare in hydrology and include tidal propagation in aquifers (Bakker 2019) and discharge generation in alpine catchments (Schaefli and Zehe 2009). Also in these cases, a sensitivity analysis performed isolating the processes (and hence the parameters) contributing to different temporal scales can be beneficial to enhance parameter identifiability.

The paper is structured as it follows. In the methodology section, we briefly introduce the Sobol indices, the continuous and discrete wavelet transforms, addressing the interested reader to more specific literature for further information. Then, we introduce the four sensitivity analysis approaches, how we compare them and we describe the hydrological problem that we consider as case study. Considering the large amount of results that we could show, we present a selection of the most relevant ones, focusing on the first order Sobol indices, and we provide as supporting material the results computed for the total Sobol indices. We critically discuss the results considering the effect of the sample size used to compute the sensitivity indices and hence the convergence of the sensitivity

indices, the effect of the chosen range of variability for the model parameters, focusing in particular on the amplitude of the signal and on the effect of a Gaussian noise on the synthetic observations (representing a measurement error), and the advantages and disadvantages of the wavelet-based sensitivity analysis methods.

2 Methodology

The goal of global sensitivity analysis can be for example to evaluate how much of the uncertainty in the model outputs depends on the uncertainty in the model input parameters, including their interaction, or to rank the model parameters according to their sensitivity. In this work, we focus on the use of variance based indices, i.e., the Sobol index, to achieve these goals, however other metrics are also available (Dell'Oca et al. 2017) and could be similarly applied. The novelty in the proposed methodology is the calculation of the sensitivity indices considering wavelet decomposition of the objective function. Such approach is not limited to the calculation of the Sobol index, but can be easily extended to other common metrics (e.g., Morris method (Smith 2013)) applied in hydrological problems where the parameter space has high dimensionality (Merchán-Rivera et al. 2022).

2.1 Sobol indices

We consider a scalar model $Y = f(X_i)$ which depends on X_i parameters with $i = 1 \ldots k$ (Saltelli et al. 2010). The derivation of the Sobol indices is based on the decomposition of the variance of the model output into terms which can be attributed to each parameter X_i, as well as to the effect of their interactions (Smith 2013). For example, for each parameter, we can write the model variance based first order effect as $V_{X_i}\left(E_{\boldsymbol{X}_{\sim i}}\left(Y|X_i\right)\right)$, where $\boldsymbol{X}_{\sim i}$ is the matrix of all parameters except X_i.

The first-order Sobol index for the parameter X_i is defined as

$$S_i = \frac{V_{X_i}\left(E_{\boldsymbol{X}_{\sim i}}\left(Y|X_i\right)\right)}{V(Y)} \tag{1}$$

and represents the proportion of variance of the model $V(Y)$ explained by the varying X_i alone and averaging over variations in other input parameters.

The total effect of X_i is quantified by the total Sobol Index, defined as

$$S_{Ti} = \frac{E_{\boldsymbol{X}_{\sim i}}\left(V_{X_i}\left(Y|\boldsymbol{X}_{\sim i}\right)\right)}{V(Y)} = 1 - \frac{V_{\boldsymbol{X}_{\sim i}}\left(E_{X_i}\left(Y|\boldsymbol{X}_{\sim i}\right)\right)}{V(Y)} \tag{2}$$

and quantifies the contribution of the parameter X_i to the total output variance of the model Y, including all interactions of the parameter X_i with the other model parameters.

Together, the total variance of the model output equals the sum of all terms in which the variance can be decomposed. More details about the mathematical derivation of the Sobol indices can be found in Smith (2013).

2.2 Continuous wavelet

Wavelet transform permits to determine the relevant scales of variability of a signal and to highlight the changes in the modes of variability within a time series. The continuous wavelet transform (CWT) of a discrete sequence d, with constant time spacing δt, is defined as its convolution with a scaled and translated version of the mother wavelet $\psi_0(\eta)$:

$$W_{n\prime}(s) = \sum_{n=0}^{N-1} d_n \psi^* \left[\frac{(n\prime - n)\delta t}{s}\right] \tag{3}$$

where (*) indicates the complex conjugate, n is the localized time index, $n\prime$ is the time variable, s is the wavelet scale and N is the length of the data series. In this paper, the Morlet wavelet was chosen as mother wavelet (Labat 2010). Generally, the wavelet transform $W_{n\prime}(s)$ is complex, hence one can identify an amplitude $\left|W_{n\prime}(s)\right|$ and a phase $\tan^{-1}\left[\Im\left\{W_{n\prime}(s)\right\}/\Re\left\{W_{n\prime}(s)\right\}\right]$. The wavelet power spectrum is defined as

$$l_n(s) = \left|W_{n\prime}(s)\right|^2 \tag{4}$$

And the cumulative wavelet-periodogram is then defined as.

$$C_n(s) = \sum_{k=s_0}^{s} l_n(k), \text{with} = s_0, \ldots, s_{max}(n) \tag{5}$$

where $s_{max}(n)$ is the maximum scale analyzed at each step outside the so called cone of influence (COI), which is the region of the power spectrum where boundary effects are important. The CWT in fact assumes to have cyclic data and hence infinite time series. Since this is not the case in practice, the wavelet transformation at the beginning and end of the time series may contain some errors due to side effects. More details about the CWT can be found in Torrence and Compo (1998).

2.3 Discrete wavelet

As a difference to the continuous wavelet transform, the discrete wavelet transform (DWT) analyses signals intro progressively finer octaves, hence operating on scales with discrete numbers, typically based on integers power of two. This allows us to reconstruct the signal in a much easier and efficient way. The DWT is defined as

$$\psi_{j,k}(t) = 2^{-j/2}\psi\left(2^{-j}t - k\right) \tag{4}$$

where $\psi(t)$ is the mother wavelet function, j is the translation index, and k is the dilatation index. In our work, we used the Haar wavelet. More about DWT can be found in Heil and Walnut (1989).

2.4 Methods applied to perform the sensitivity analysis

In this paper, we considered four approaches to perform the sensitivity analysis and our model is defined as $Y = f(X_i)$. The workflow of the four methods is illustrated in Fig. 1. Scope of the comparison of multiple methods is to show that also parameters that may seem non influent with a classical Sobol analysis (Method 1) performed in the time domain may actually be important in the wavelet domain (Methods 2, 3 and 4). This is particularly interesting in hydrology where the variability in the observations is often caused by the superposition of multiple signals with different relevant temporal scales (Labat 2010). For example, a river influenced by the management of a hydropower plant is typically affected by signals with different frequencies (Ciria et al. 2019; Zolezzi et al. 2009), which propagate towards the aquifer and affect surface-water groundwater interaction.

2.4.1 Method 1 (MAE): Sobol index in the time domain

The first method considers as objective function for the calculation of the Sobol index the mean absolute error (MAE) computed in the time domain, defined as

$$\mathrm{MAE}(O(t), y(t, \boldsymbol{X})) = \frac{\sum_{t=1}^{N} |O(t) - y(t, \boldsymbol{X})|}{N} \tag{5}$$

where N indicates the length of the vector of some observed values $O(t)$ of a time dependent variable and $y(t, \boldsymbol{X})$ represents the corresponding modelled values. The MAE is a classical metric for the evaluation of the goodness of fit of hydrological model, in particular in the context of surface water-groundwater interaction (Serrano and Workman 1998). Method 1 represents therefore our benchmark since it represents a commonly applied sensitivity analysis approach. We further considered other objective functions, such as the root mean squared error, however we did not observe significant differences in the results and therefore we consider in this work only Eq. (5).

2.4.2 Method 2 (DWT): Sobol index computed for each DWT level

In Method 2, we considered for the Sobol index calculation the MAE computed considering each single level in which the observed and the modelled time series can be decomposed. Therefore, for each level in which we decompose the two signals of observed and modelled time series we compute the MAE according to Eq. (5) and then we calculate the first order and the total Sobol indices according to Eqs. (1) and (2), respectively. Beside the MAE we tested the root mean squared error without observing significant differences in the results.

In Method 2, therefore, we decompose both the synthetic observations and the model results with the DWT, we compute the MAE on each level and then apply the Sobol

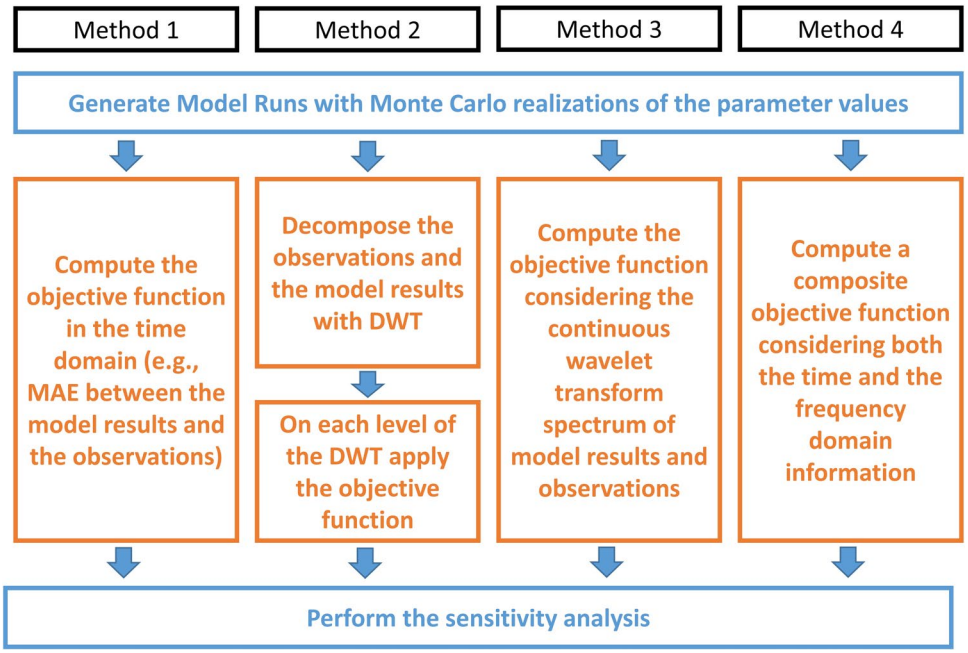

Fig. 1 Description of the process to perform the sensitivity analysis using the four methods considered in this work. Blue indicate the parts of the process in common among the four methods, in orange we highlight the differences

Indices. Therefore, each model parameter is characterized by a set of sensitivity indices equal to the number of levels in which the signal is decomposed using the DWT. This approach aims to disentangle the superimposed signals and hence focuses on the dominant parameters controlling the processes occurring at different temporal scales. Notice that the scale dependent sensitivity indices of Method 2 are novel information that is not equivalent to the sensitivity indices for the full signal. In particular, the sum of the scale dependent sensitivity indices does not converge in general to the sensitivity indices computed for the full signal. In fact, for the i-th first order Sobol indices we have

$$S_i = \frac{V_i}{var\left[f(\boldsymbol{X})\right]} = \frac{\sum_j V_i^{\{j\}} + \sum_{j\neq k} V_i^{\{jk\}}}{\sum_{jk} cov\left[f_j(\boldsymbol{X}), f_k(\boldsymbol{X})\right]} \tag{6}$$

The second term in the numerator is a covariance term reflecting the interscale dependency where j and k denote the scales and can be expressed as:

$$\sum_{j\neq k} V_i^{\{jk\}} = \sum_{j\neq k} \left(E_{\boldsymbol{X}_{\sim i}}\left[f_j(\boldsymbol{X})|\boldsymbol{X}_i\right] - E_{\boldsymbol{X}_i}\left[E_{\boldsymbol{X}_{\sim i}}\left[f_j(\boldsymbol{X})|\boldsymbol{X}_i\right]\right]\right) \cdot \left(E_{\boldsymbol{X}_{\sim i}}\left[f_k(\boldsymbol{X})|\boldsymbol{X}_i\right] - E_{\boldsymbol{X}_i}\left[E_{\boldsymbol{X}_{\sim i}}\left[f_k(\boldsymbol{X})|\boldsymbol{X}_i\right]\right]\right) \tag{7}$$

The term expressed by Eq. 7 is generally different form 0 and therefore the sum of the first order Sobol indices computed at each level $\sum_j V_i^{\{j\}}$ is not equal to the first order Sobol indices computed for the entire signal.

Hence the i-th first order Sobol indices can be rewritten as:

$$\begin{aligned} S_i &= \frac{V_i}{var\left[f(\boldsymbol{X})\right]} = \frac{var_{\boldsymbol{X}_i}\left[E_{\boldsymbol{X}_{\sim i}}\left[f(\boldsymbol{X})|\boldsymbol{X}_i\right]\right]}{var\left[f(\boldsymbol{X})\right]} \\ &= \frac{\sum_{jk} cov_{\boldsymbol{X}_i}\left[E_{\boldsymbol{X}_{\sim i}}\left[f_j(\boldsymbol{X})|\boldsymbol{X}_i\right], E_{\boldsymbol{X}_{\sim i}}\left[f_k(\boldsymbol{X})|\boldsymbol{X}_i\right]\right]}{\sum_{jk} cov\left[f_j(\boldsymbol{X}), f_k(\boldsymbol{X})\right]} \end{aligned} \tag{8}$$

2.4.3 Method 3 (R): Sobol index computed for the Wavelet Periodogram Efficiency criterium

Method 3 is based on the Wavelet Periodogram Efficiency criterium $R(O, y)$ as presented by Schaefli and Zehe (2009) for the calculation of the Sobol index. The Wavelet Periodogram Efficiency criterium is a measure to quantify the similarity between two wavelet periodograms and, in particular, to compare their distribution over all scales at each time step t. The Kolmogorov–Smirnov distance at time step t is defined as

$$D_n(t|O(t), y(t,\boldsymbol{X})) = max\left|\frac{C_n(t,s|O(t))}{C_n\left(t, s=s_{max}|O(t)\right)} - \frac{C_n(t,s|y(t,\boldsymbol{X}))}{C_n\left(t, s=s_{max}|y(t,\boldsymbol{X})\right)}\right| \tag{9}$$

where $y(t,\boldsymbol{X})$ is again a realization of the model with parameters $\boldsymbol{X}$ and $O(t)$ the set of the observed time series. The overall wavelet periodogram efficiency criterion is then obtained averaging $D_n(t)$ over all time steps:

$$R(O(t), y(t,\boldsymbol{X})) = \frac{1}{N}\sum_{t=1}^{N} D_n(t|O(t), y(t,\boldsymbol{X})) \tag{10}$$

R varies between 0 and 1, and a smaller value indicates a better fit between $y(t,\boldsymbol{X})$ and $O(t)$.

Considering R as objective function for the Sobol index allows us to give a particular attention to the frequency composition of the signal, but the information is aggregated for the entire signal and one single index is calculated for each model parameter. Method 3 therefore significantly differs from Method 2 since the information contained at different scales is merged together in the objective function R¸ while in Method 2 we obtain different sensitivity indices for each level of the DWT.

2.4.4 Method 4 (MAER): Sobol index for a composite objective function

Method 4 considers as objective function for the calculation of the Sobol index for a combination of the MAE in the time domain and of the Wavelet Periodogram Efficiency criterium in the wavelet domain, defined as

$$\mathrm{MAER}(O(t), y(t,\boldsymbol{X})) = \frac{\sum_{t=1}^{N}|O(t) - y(t,\boldsymbol{X})|}{N} + \frac{1}{N}\sum_{t=1}^{N} D_n(t|O(t), y(t,\boldsymbol{X})) \tag{11}$$

MAER aims at considering both the relevance of scale dependent processes by using R and their relevance in absolute terms on the modelled signal by using the MAE.

2.5 Convergence analysis

As stated by Sarrazin et al. (2016), there are several kinds of convergence analysis that can be performed in the context of sensitivity analysis. For example, the convergence of

the input factor screening aims at identifying which are the most influent parameters; The convergence of the input factor ranking is reached when the ranking of the parameters is stable independently on the increasing number of samples used for the calculation of the sensitivity analysis. The convergence of the sensitivity indices values aims at identifying the minimum number of samples needed to obtain a constant value in the calculated sensitivity indices. The choice of which kind of convergence should be reached depends on the goal of the sensitivity analyses, and it is often a compromise between the computational resources available and the precision needed. In our case, we say that convergence has been reached, if the change in the Sobol Indices from one simulation to the one with more samples is smaller than 10%. The number of samples needed to reach the convergence varies as a function of several aspects, as for example the model itself and the number of model parameters. In this work, we created a set of 10^6 samples for each model configuration that we analyzed. For each of these sets of parameters we than randomly choose 10^3, 10^4 and 10^5 samples to create smaller sets of realizations and to evaluate if any difference is present among the four methods in terms of convergence.

The four methods to perform the sensitivity analysis are applied to a hydrological model. The value of the Sobol indices are used also to identify the non-sensitive parameters (screening) and the ranking of the most sensitive parameters.

2.6 Application to a hydrological problem

An appropriate case study to identify advantages and limitations of the proposed methodology is to consider hydrological problems characterized by the superposition of periodic signals. Among them we can mention streamflow generation in alpine catchments (Schaefli and Zehe 2009) as well as in karst systems (Bittner et al. 2021a). Such problems are however characterized by high parameter space dimensionality and therefore sensitivity analysis is rarely performed considering Sobol indices. Other relevant problems which are characterized by a low parameter space dimensionality and by the availability of analytical solutions are the propagation of tides in groundwater (Bakker 2019; Slooten et al. 2010), the propagation of natural river stage fluctuations towards the aquifer (Serrano and Workman 1998) as well as the propagation of hydropeaking waves in groundwater (Hucks Sawyer et al. 2009). Such analytical solutions are widely used in practice to estimate lumped model parameters.

We consider a 1-dimensional, homogeneous, semi-infinite aquifer, whose water level is affected by the periodic stage fluctuations of an adjacent river. As reported in Hucks Sawyer et al. (2009), the transient flow in the aquifer is described by the 1-dimentional linearized Boussinesq equation

$$\frac{\partial h}{\partial t} = P\frac{\partial^2 h}{\partial x^2} \tag{12}$$

where h is the hydraulic head [m], x is the spatial coordinate [m] and t is the time [d]. P is the aquifer diffusivity [m^2/d] and it is related to the aquifer properties:

$$P = \frac{Kb}{s_y} \tag{13}$$

where K is the hydraulic conductivity [m/d], s_y is the specific yield [-] and b is the saturated aquifer thickness [m].

The boundary conditions considered state that at the river bank ($x=0$), the groundwater fluctuations correspond to the river fluctuations, while at large distance from the river the lateral flow approaches zero. The analytical solution of Eq. 14 in a semi-infinite aquifer is derived following Singh (2004). We consider that the river fluctuations may be described by the superposition of two sinusoidal waves: $h_1(x=0,t) = A_1\sin(\omega_1 t)$ and $h_2(x=0,t) = A_2\sin(\omega_2 t)$, where ω_1 and A_1 are the frequency and amplitude of the first sinusoidal wave, respectively, and ω_2 and A_2 are the frequency and amplitude of the second sinusoidal wave, respectively. The second wave is assumed to have smaller amplitude and higher frequency respect to the first one. Moreover, we consider that both $h_1(x=\infty,t)=0$ and $h_2(x=\infty,t)=0$. The fluctuations in the aquifer are hence described by:

$$\begin{aligned} h(x,t) =& A_1\exp\left(-x\sqrt{\frac{\omega_1}{2P}}\right)\sin\left[-x\sqrt{\frac{\omega_1}{2P}}+\omega_1 t+\phi\right] \\ &+ A_2\exp\left(-x\sqrt{\frac{\omega_2}{2P}}\right)\sin\left[-x\sqrt{\frac{\omega_2}{2P}}+\omega_2 t+\phi\right] \end{aligned} \tag{14}$$

where ϕ is a phase term [-], which is assumed to be 0 in this study.

We investigate three scenarios, S_1, S_2 and S_3, in which the amplitude A_2 represents 20%, 40% and 80% of A_1, respectively, as shown in Fig. 2. P depends on the characteristics of the aquifer, which are generally poorly known and hence uncertain. A similar signal to the one represented in Fig. 2 can be found in rivers influenced by the management of hydropower plants. In fact, this usually introduces in the river different kind of fluctuations, such as a daily fluctuation, due to the different energy demand during the day, and a weekly fluctuation, due to the lower energy demand during the weekend respect to the working days. However, this pattern can differ depending on the management of the hydropower plant, on the energy market and legislative framework leading to an uncertainty in the model parameters describing the river stage fluctuations.

We use Eq. 16 to generate synthetic observation of the groundwater level (Fig. 2). The parameters used for the

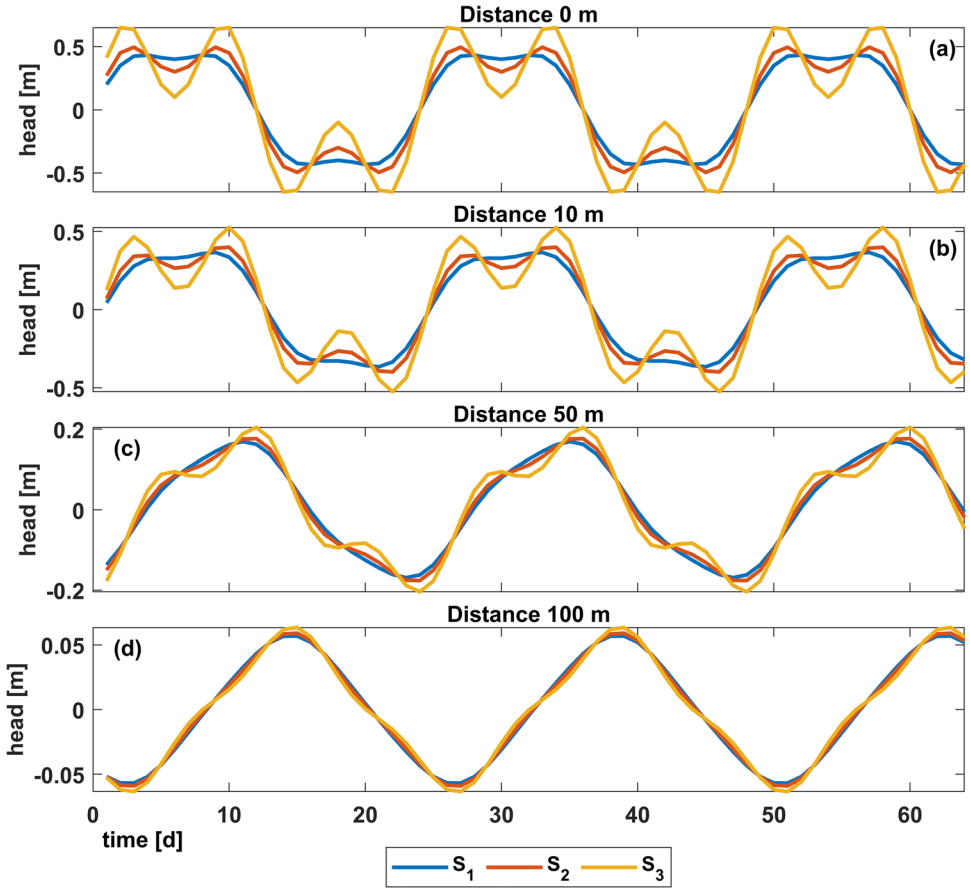

Fig. 2 Observations generated considering three scenarios for the amplitude A2: blue line S_1 (A2 = 0.2A1), red line S_2 (A2 = 0.4A1), yellow line S_3 (A2 = 0.8A1)

Table 1 Parameters considered in the sensitivity analysis

Parameter	Value for the generation of the observations	Paramenter range for the sensitivity analysis	
		From	To
P	270 m^2/d	0.27 m^2/d	2700 m^2/d
A_1	0.5 m	0.1 m	1 m
ω_1	1 cycles/d	0.5 cycles/d	1.5 cycles/d
$A_{2,S1}$	0.1 m	0.02 m	0.2 m
$A_{2,S2}$	0.2 m	0.04 m	0.4 m
$A_{2,S3}$	0.4 m	0.08 m	0.8 m
ω_2	3 cycles/d	1.5 cycles/d	4.5 cycles/d

We report their value used for the generation of the observed time series and their ranges for the calculation of the sensitivity analysis

generation of the synthetic observations with a length of 64 time points, corresponding to one measurement per hour, are reported in Table 1. Considering the length of the time series considered, we decompose the signal up to level 5 with the DWT. We can observe that the difference between S_1, S_2 and S_3 decreases with increasing distance due to the exponential decay term which dampens high frequency fluctuations at higher distances.

We also tested what is the effect on the sensitivity analysis of a Gaussian noise (measurement error) with zero mean and three different values for the standard deviation σ (i.e., 0.01m, 0.05m and 0.1m) which is added to Eq. 4 (Fig. 3).

In this study, we investigate the sensitivity of the parameters A_1, P, ω_1, A_2, ω_2 at three different distances from the river: 10 m, 50 m and 100 m, using the four methods described in Sect. 2.7. For these parameters, we chose a uniform distribution with ranges reported in Table 1.

3 Results and discussion

The four methods are tested on synthetic data, however, as shown in Huck Sawyer et al. 2009, the analytical solution that we apply is able to reproduce fairly well experimental observations in the Colorado river. Therefore, in order to illustrate the methodology, we use synthetic data, instead of experimental data to avoid the influence of model conceptual uncertainty (e.g., the representation of surface water-groundwater interaction considering negligible resistance between river and groundwater flow) and uncertainty due to boundary

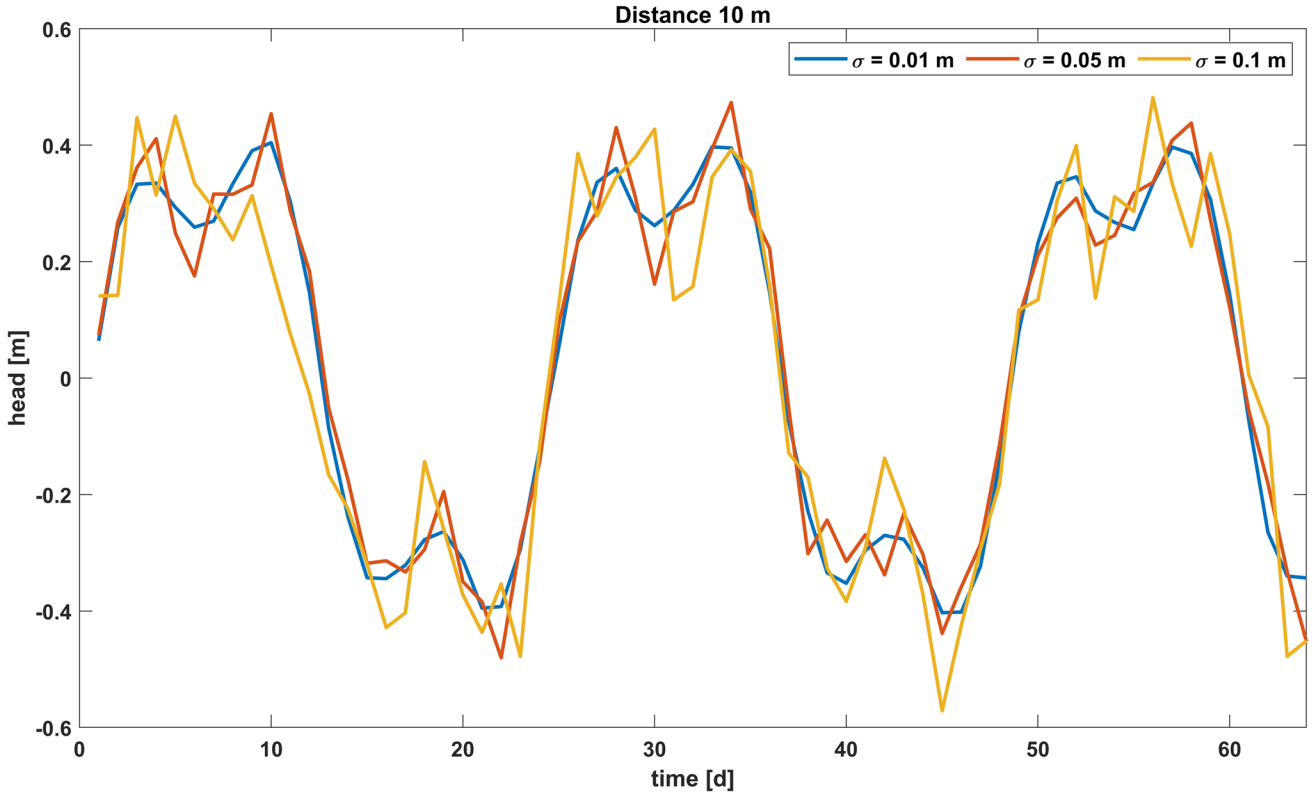

Fig. 3 Observations generated considering three standard deviations to represent the Gaussian measurement error: blue line σ = 0.01m, red line σ = 0.05m, yellow line σ = 0.1m

conditions (e.g., fix head conditions on the opposite side than the river) on the analysis of parametric uncertainty.

Considering the large amount of simulations and generated results, in the following we will focus on the most relevant aspects of the analysis. Table 2 summarizes the setups that we investigated for a specific purpose. If not explicitly mentioned, there is no remarkable difference among the results presented in the following sections and the results obtained for the other setups. The results of Method 1 are indicated with MAE, the results for the five levels of Method 2 are indicated with L1, L2, L3, L4 and L5 according to the level considered, the results of Method 3 are indicated with R and finally the results of Method 4 are indicated as MAER.

3.1 Convergence analysis

Figure 4 displays the value of the first order Sobol indices for the five model parameters considering the four different methods applied in this study and using four sample sizes (10^3, 10^4, 10^5 and 10^6realizations of parameter sets). We show the results only for S_3 ($A_2 = 0.8A_1$), no measurement error and the distance of 50 m from the river. We can observe that the value of the Sobol indices is already very similar between 10^5 and 10^6 samples, however for the

Table 2 Overview of the setups investigated in this work

Setup Purpose	Number of samples	Distance from the river	Relative amplitude of A2	Measurement error (standard deviation)
Convergence analysis	10^3, 10^4, 10^5, 10^6	50m	$0.8A_1$	0
Identify the effect of different relative amplitudes on the sensitivity indices	10^6	10m, 50m 100m	S_1 ($A_2 = 0.2A_1$) S_2 ($A_2 = 0.4A_1$) S_3 ($A_2 = 0.8A_1$)	0
Effect of measurement error on the sensitivity analysis	10^6	10m	$0.4A_1$	0.01, 0.05, 0.1

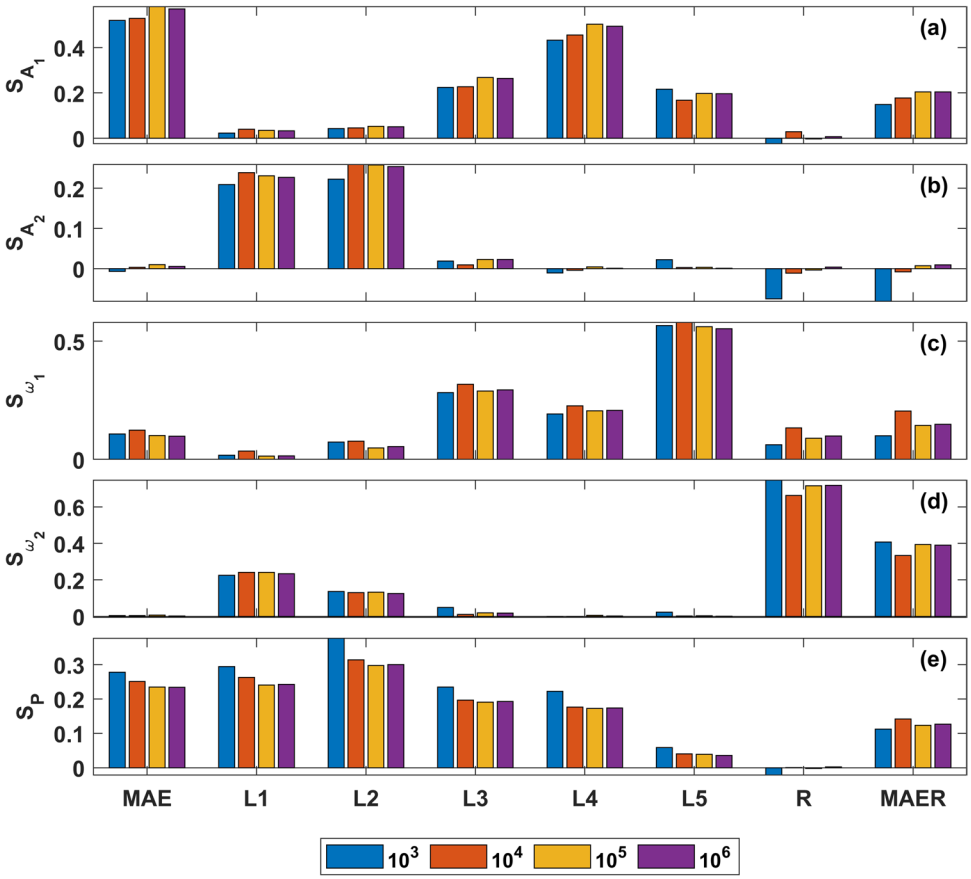

Fig. 4 First order sensitivity indices computed for different sample sizes 10^3 (blue bars), 10^4 (red bars), 10^5(yellow bars) and $10.^6$ (purple bars) for the five model parameters: A_1 (panel a), A_2 (panel b), ω_1 (panel c), ω_2 (panel d), P (panel e)

following analyses, we will consider the results obtained considering 10^6 samples. In fact, in particular for Method 2, where we compute the Sobol indices for five DWT levels, we can still observe some small differences between the results for 10^5 and 10^6 samples, in particular for Level 1 and Level 2, corresponding to the high frequency components of the signal. These differences are however insignificant for the purpose of parameter identification and ranking.

The convergence analysis performed in this work is quite simple and its purpose is only to identify the sample size to be used for further analysis. More rigorous approaches, as discussed for instance in Sarrazin et al. (2016) may be needed depending on the purpose of the study. We can observe however that among the four methods the convergence is very similar. Considering the computational time, Method 2 is more expensive than the others because it requires the decomposition of the signal and the sensitivity analysis for each level considered. The additional computational effort is related to the computational cost of the DWT and CWT in methods 2, 3 and 4, which depends on the length of the time series. This additional time can represent a minimal fraction of the total computational effort for complex hydrological models. In our case, however, since we are dealing with an analytical solution, the increase in computational time with respect to method 1 varies between a factor of two (method 3 and 4) and a factor of five (method 2). The results are shown only for the first order Sobol index, but a similar pattern is present also in the analysis of the total Sobol indices (Figure S1 in the supporting information).

3.2 Identify the effect of different relative amplitudes on the sensitivity indices

Hydropeaking waves can be characterized by different amplitudes at multiple temporal scales depending on the management of the hydropower plants, the legislation and the catchment. Therefore, we investigate three different scenarios in which the range in the amplitude of the high frequency wave A_2 varies (see Table 2 and Fig. 1). The results are presented separately for Method 2 (Fig. 5) and the other three methods (Fig. 6), to better appreciate the advantage of performing a scale dependent sensitivity analysis for each DWT level in which the signal can be decomposed.

We can observe that the sensitivity indices for L1 and L2 are very different in comparison to higher levels and indicate that A_2 and ω_2 can be identified by considering these levels in the signal, independently on the relative amplitude of A_2. It is interesting to notice that, the higher A_2, the more the

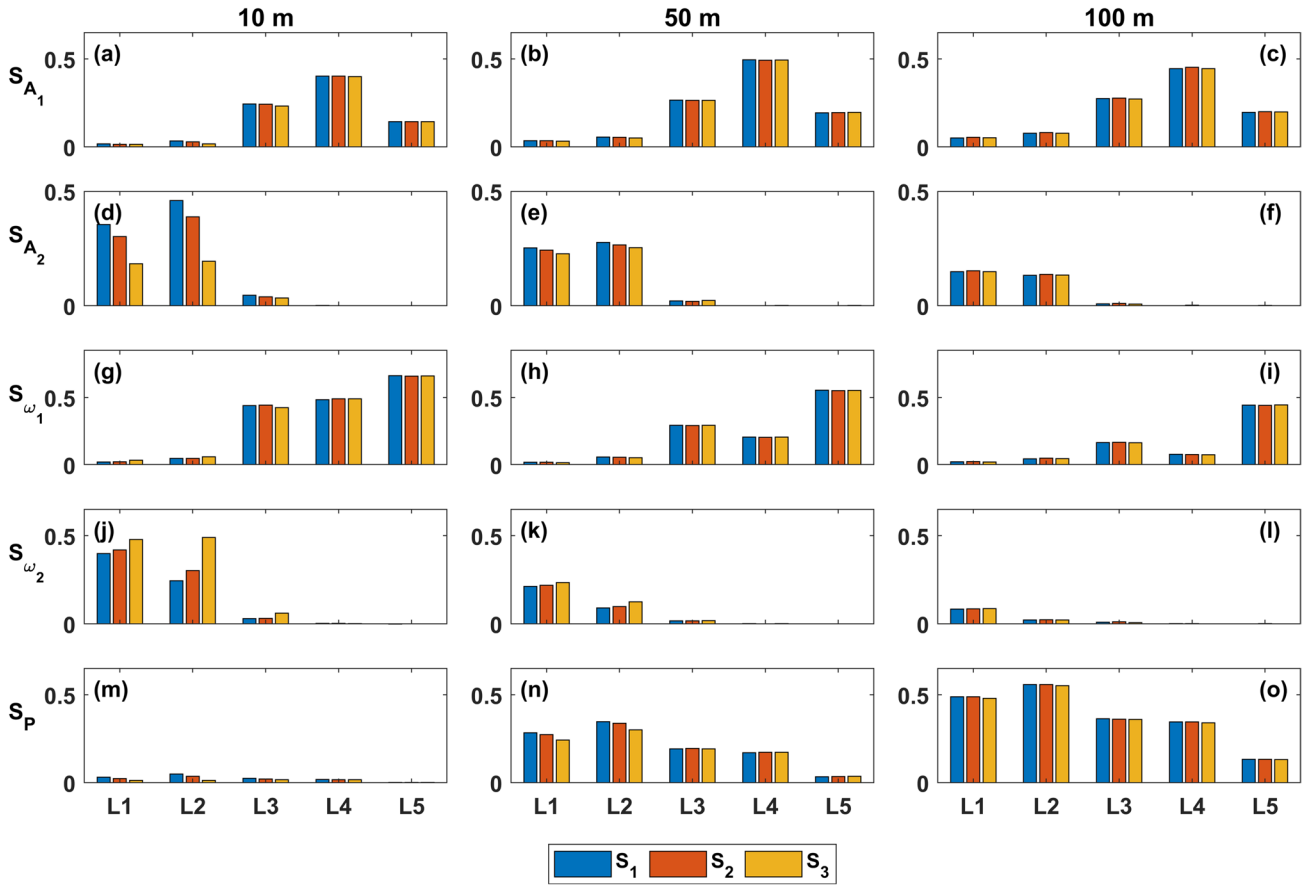

Fig. 5 First order sensitivity indices computed considering three scenarios for the amplitude A_2 using Method 2: blue bars S_1 ($A_2 = 0.2A_1$), red bars S_2 ($A_2 = 0.4A_1$), yellow bars S_3 ($A_2 = 0.8A_1$)

sensitivity of ω_2 increases, while the sensitivity of A_2 itself decreases.

To identify A_1 and ω_1, it is appropriate to select L3 to L5. Comparing the results for the three different distances, we can observe that A_2 and ω_2 are relevant parameters at short distanced from the river, consistently with the fact that the aquifer acts as a low pass filter for the river fluctuations (Fig. 1). The diffusivity of the aquifer P becomes the most relevant parameter at 100m distance from the river considering L1 and L2, while considering L3, L4 and L5, the parameters A_1 and ω_1 have similar or even higher sensitivity values than P.

Figure 6 shows that the sensitivity analysis based on the MAE, is not able to identify the parameter ω_2 at any distance from the river. If we include information about the scale dependence of the investigated processes by considering R both in Method 3 and in Method 4, we can observe that ω_2 is sensitive and the sensitivity decreases with increasing distance from the river. The sensitivity of P increases with increasing distance from the river and the parameter is sensitive only if the MAE is considered in the objective function used for the sensitivity analysis (Method 1 and Method 4). The sensitivity of A_2 is very small compared to the other parameters in all three approaches presented in Fig. 6.

Summarizing, independently on the relative amplitude of A_2, Method 1 is not able to identify A_2 and ω_2 as sensitive parameters. The reason for that, is that their contribution to the MAE is not large since the rapid water table fluctuations are present only at short distances and they are relatively small in comparison to A_1. Method 2 is able to identify as sensitive all five model parameters, depending on the distance and the level considered in the analysis. The decomposition in the different scales allows us to focus on relevant processes with a characteristic frequency and moreover it allows us to detect the sensitivity of P for distances in which the periodicity in the groundwater fluctuations is not very relevant anymore due to the exponential decay of their amplitude. Method 3 identifies only ω_1 and ω_2 as sensitive parameters, because the objective function is completely biased towards the information in the frequency domain. Finally, Method 4 is able to identify A_1, ω_1, ω_2 and P as sensitive parameters because it considers an objective function that combines MAE and R. In this case, depending on the need of the

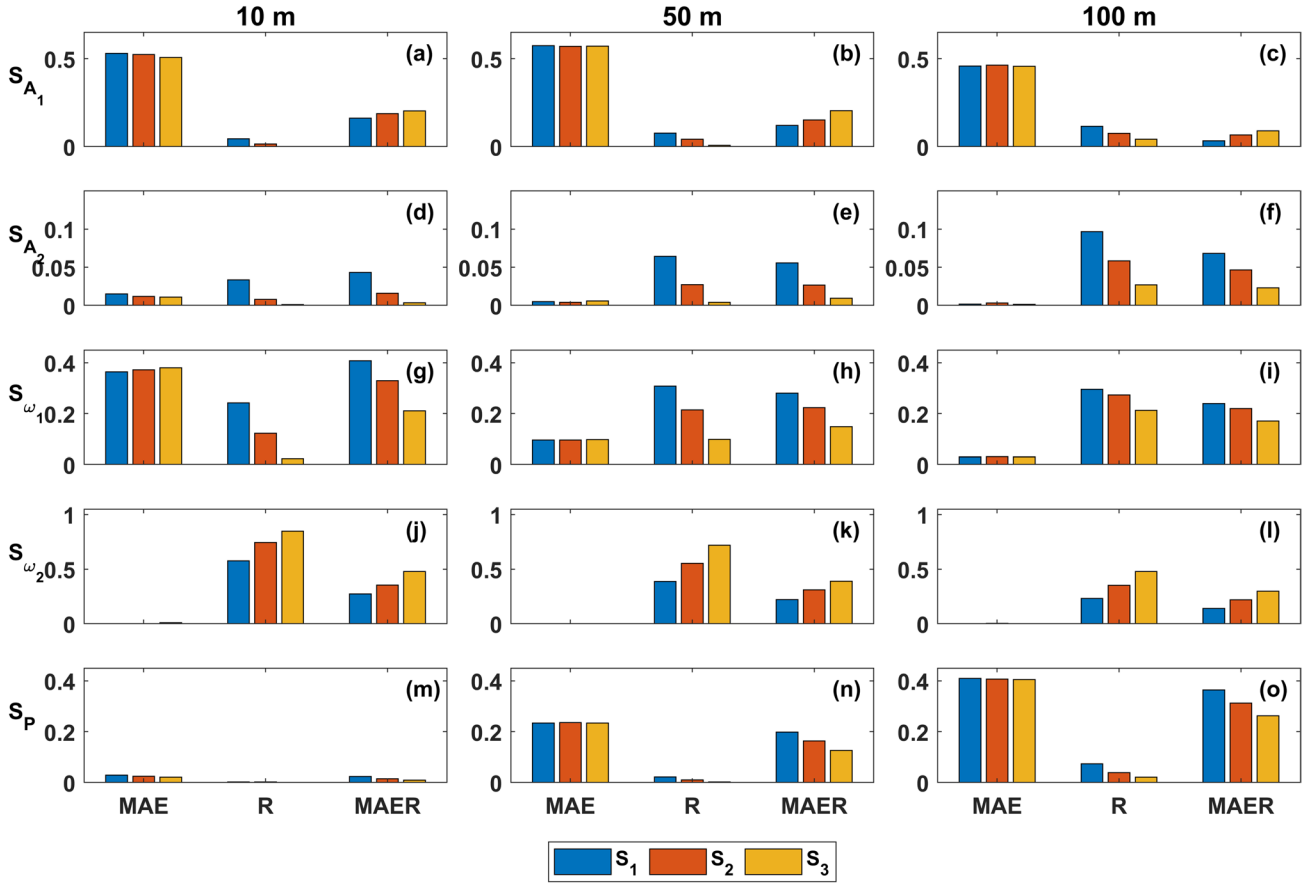

Fig. 6 First order sensitivity indices computed considering three scenarios for the amplitude A_2 using Method 1(MAE), 3 (R) and 4 (MAER): blue bars S_1 ($A_2 = 0.2A_1$), red bars S_2 ($A_2 = 0.4A_1$), yellow bars S_3 ($A_2 = 0.8A_1$)

analysis, it is also possible to use different weights to MAE and R, however, considering the pattern observed in Fig. 6, the identification of A_2 will remain challenging using this method as neither MAE nor R identify A_2 as very sensitive parameter. Although computationally more expensive than the other methods, Method 2 allows us to increase the parameter identifiability. While the results are shown only for the first order Sobol index, a similar pattern is obtained also for the total Sobol indices (Figure S2 and Figure S3 in the supporting information).

Both Figs. 5 and 6 show the interaction between parameters A_2 and ω_2, in the methods in which those parameters are sensitive. In fact, the increase in the relative value of A_2 leads to a higher sensitivity in ω_2. This means that the larger is the fluctuation of the river stage at high frequency, the more relevant is the identification of the right frequency for the objective function. This effect is illustrated in Fig. 7 considering even the MAE as objective function, where the sensitivity of A_2 is small for a distance of 10m from the river and the scenario S_2 (where $A_2 = 0.4A_1$), and evidenced by the behavior of its derivatives with respect to A_2 and ω_2. In particular, we can observe the much larger increase in MAE by changing ω_2 in comparison to its increase by varying A_2.

3.3 Effect of measurement error on the sensitivity analysis

This analysis focuses on the effect of a Gaussian measurement error on the results of the sensitivity analysis. The values of the first order Sobol index are barely affected by the measurement error using the Method 1. When we start considering the analysis which include information from the wavelet decomposition (Methods 2, 3 and 4), we can observe some effects on the value of the first order Sobol index of the parameters. However, the effect is not large and it does not influences the ranking of the sensitive parameters which remains the same independently on the error. The sensitivity of different parameters is affected by the measurement error while considering different methods and a clear pattern

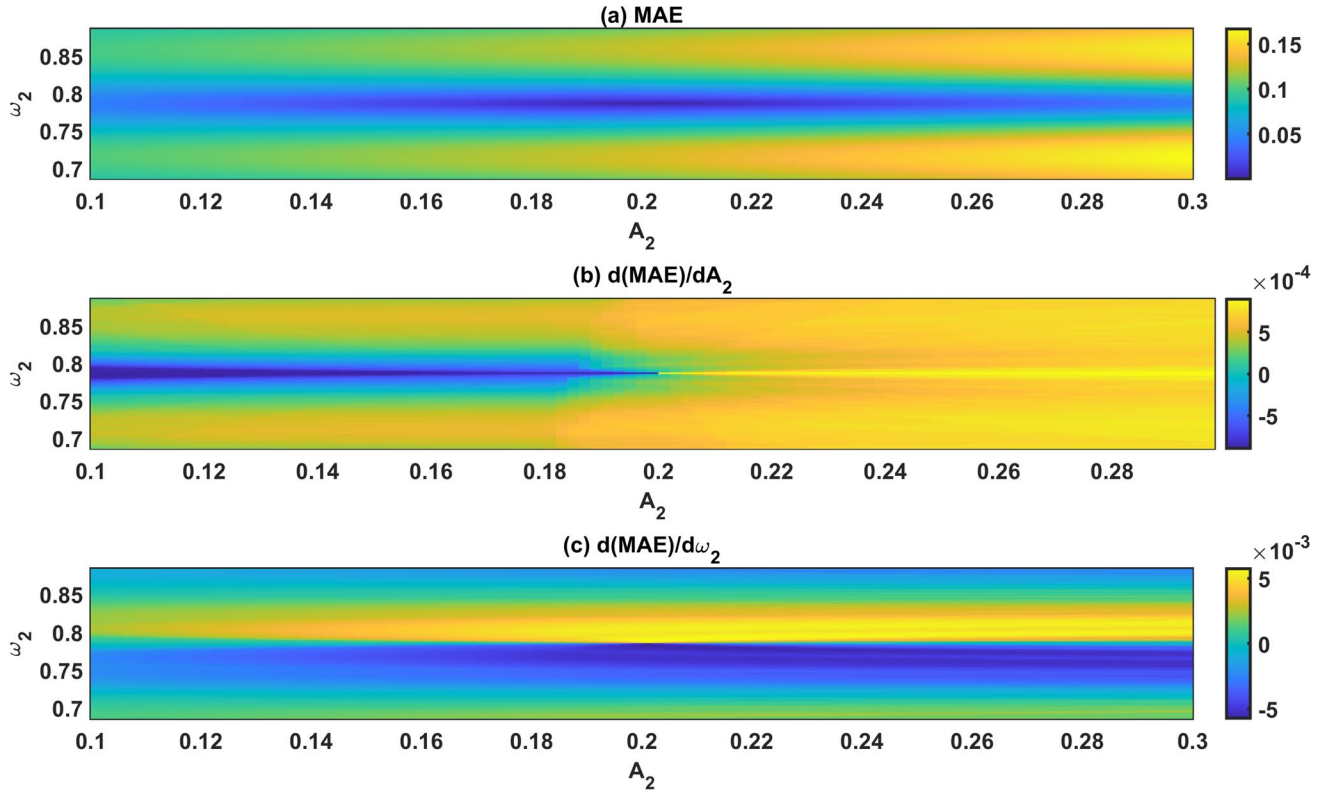

Fig. 7 MAE computed varying only A_2 and ω_2, while keeping constant all other parameters. The second and the third panel, represent the $\frac{d(MAE)}{dA_2}$ and $\frac{d(MAE)}{d\omega_2}$, respectively

cannot be identified. Therefore, we can conclude that the results obtained using Method 1 are slightly more stable than the results obtained with the other methods if a Gaussian measurement error affects the objective function, although, at least for the example investigated in this study, this effect seems to be negligible for the identification and the ranking of sensitive model parameters (Fig. 8).

3.4 Implication for parameter estimation

The implications for parameter estimation are illustrated considering a simple Quasi-Newton Algorithm to find the optimal solution that minimizes the objective functions. We consider a set of fixed parameters (Table 3), which are used as values for the parameters that are not sensitive according to the result of the sensitivity analysis performed with the four different methods and also as starting points for the optimization algorithm. We consider a distance of 10 m from the river and no measurement error. The results are reported in Table 3. In addition to the results for Method 1 to Method 4, we also consider the mean value of the sensitive parameters for Method 2 computed over different scales. Specifically, A_1 and ω_1 are the mean value of L3, L4 and L5, A2 and ω_2 are the mean value of L1 and L2, and P is not optimized. Moreover, we consider a composite objective function for the optimization problem after performing the sensitivity analysis with Method 2 where we minimize the sum of the MAE computed at each level. These are to some extent arbitrary choices, as we consider equally relevant all levels and the attempt to merge the different information obtained at different scales could be further investigated in future studies.

We can observe that the most convenient method in the parameter estimation exercise is Method 2, since it allows to optimize four parameters. It is also interesting to notice that the optimization algorithm converges towards similar values of the sensitive parameters for the different levels in the DWT decomposition, with the exception of A_1 at L5 which converges to a value that is the furthest apart from the true values in comparison to the other methods.

However, also Method 4 offers a very interesting alternative. In fact, by using the combined objective function it is able to identify the true frequencies, although P and A_2 are fixed to a wrong value. The parameter A_1 on the contrary is not very close to the true value. Method 3 is able to identify as expected the frequencies ω_1 and ω_2 quite accurately, while Method 1 captures relatively well ω_1 but A_1 does not converge to the right value better than Method 2 L3 and Method

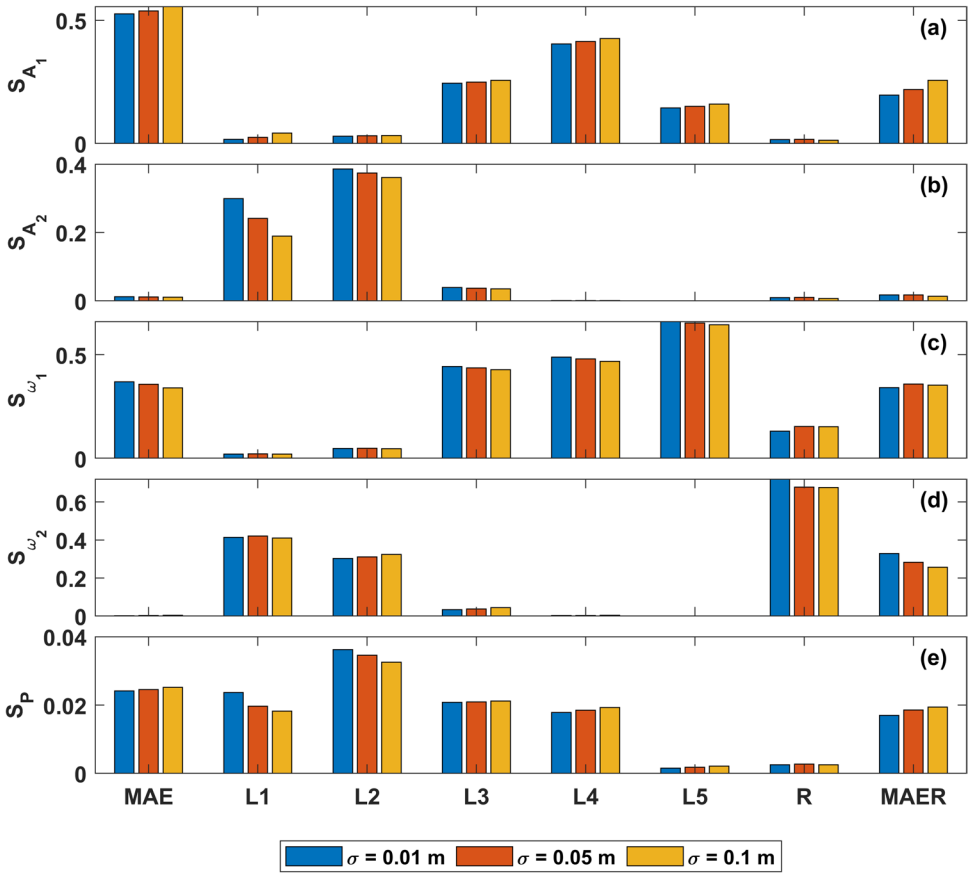

Fig. 8 First order sensitivity indices computed considering three standard deviations to represent the Gaussian measurement error: blue bars σ = 0.01 m, red bars σ = 0.05 m, yellow bars σ = 0.1 m

Table 3 Results of the parameter estimation exercise. Only sensitive parameters (number bold) are considered by the optimization algorithm

	A_1 (m)	ω_1 (1/d)	A_2 (m)	ω_2 (1/d)	P (m^2/d)
True values	0.5	0.2618	0.2	0.7854	270
Fixed parameters	0.3	0.3	0.1	0.85	40
Method 1	**0.7131**	**0.2711**	0.1	0.85	40
Method 2 L1	0.3	0.3	**0.3417**	**0.7966**	40
Method 2 L2	0.3	0.3	**0.3581**	**0.7968**	40
Method 2 L3	**0.7131**	**0.2711**	0.1	0.85	40
Method 2 L4	**0.7131**	**0.2711**	0.1	0.85	40
Method 2 L5	**0.9218**	**0.2703**	0.1	0.85	40
Method 2 Mean	**0.7827**	**0.2708**	**0.3499**	**0.7967**	40
Method 2 Composite	**0.7023**	**0.2694**	**0.3624**	**0.7987**	40
Method 3	0.3	**0.2446**	0.1	**0.7855**	40
Method 4	**0.1973**	**0.2613**	0.1	**0.7861**	40

2 L4. This indicates the importance of having also the possibility of constraining the aquifer diffusivity P, for example by taking measurements further away from the river.

Figure 9 shows that Method 1 is able to capture the low frequency variability of the groundwater table fluctuations, but systematically misses the high frequency part of the signal. Method 3 and Method 4 display a similar dynamic as the observations, but they underestimate the amplitude of the fluctuations. Considering L1 and L2 in Method 2, we have a similar result as for Method 3 and Method 4, although the amplitude is to some extent better represented, while considering L4 and L5 we obtain a signal similar to the MAE. The result obtained by the proposed averaging procedure and the composite objective function are by far the most satisfactory results as they properly capture both the frequencies and the amplitudes of the observed groundwater fluctuations, although we did not provide any optimization for P because it was not identified as a sensitive parameter.

4 Conclusion

In this work, we compared four different approaches to perform a sensitivity analysis and three of them are novel since they consider metrics defined in the wavelet domain. The motivation for considering wavelet decomposition relies in the evidence that hydrological time series are the result of processes that affect different temporal scales and therefore we aim at taking advantage of this property to enhance the parameter identifiability. Although we consider in this work a problem with low parameter dimensionality, the proposed

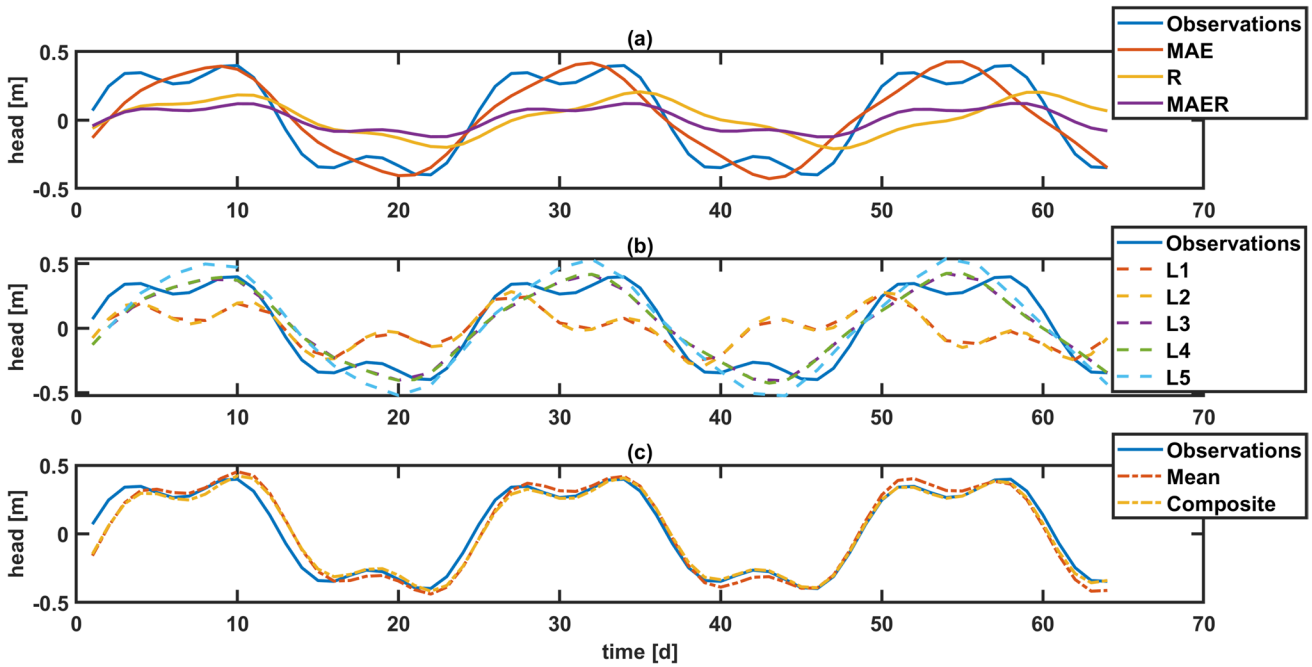

Fig. 9 Results of the optimization exercise for **a** MAE (red continuous line, first panel), R (yellow line continuous, first panel), MAER (purple continuous line, first panel), **b** L1 (red dashed line, second panel), L2 (yellow dashed line, second panel), L3 (purple dashed line, second panel), L4 (green dashed line, second panel), L5 (cyan dashed line, second panel) and **c** the mean of L1-L5 parameters (red dash-dotted line, third panel) and the parameter of the composite L1-L5 objective function (yellow dash-dotted line, third panel). Observations are the blue continuous line in all three panels

methodology is not restricted to this simple yet relevant setup. The sensitivity analysis results show that in aquifers affected by hydropeaking the properties of the wave (amplitude and frequency) are generally more relevant than the aquifer properties (hydraulic conductivity, specific yield and aquifer thickness). An accurate description of surface water management practices is therefore of utmost importance for the study of surface water-groundwater interaction in this kind of systems. If we want to extend the proposed methodology to a hydrological model focusing on discharge time series prediction in an alpine catchment, we can perform the DWT of the discharge observation and of the model results. We can compare then the results with the observation at each scale using an appropriate metric, such as the Nash Sutcliffe Efficiency. In this way, we can better identify and eventually constrain for instance the snow and glacier parameters considering daily and seasonal components of the discharge signal. Of course, if processes like snow and glacier melt share the same scales of variability, the identification of their parameters separately can remain challenging. Further work is hence needed to test the methodology in more complex and comprehensive hydrological models.

We chose a low dimensionality problem because we focus on variance-based sensitivity analysis. However, the extension to the application of the wavelet transform to other sensitivity indices (e.g., Morris method (Smith 2013)) is straightforward. Application to field measurements is beyond the scope of this paper, but it was demonstrated that the method is robust also in case of experimental errors present in the synthetic observations. The data presented in Basilio-Hazas et al. (2022) could also represent a benchmark for the application of methodology. In that case, however, the relevant periodicities are the weekly and the seasonal ones and the complexity of the aquifer system requires the use of a numerical model for the representation of the measured hydraulic heads. A Gaussian measurement error affects the value of the Sobol index computed for some parameters in the wavelet domain, but it does not affect the identification and ranking of the sensitive parameters.

The analyses highlight that the most promising method to enhance parameter identifiability is based on the discrete wavelet transform decomposition of the signal and then on the calculation of the objective function for the different scales in which the signal is decomposed. Although computationally more expensive, this method allows us to identify the maximum number of parameters in the example considered in this study. This information can be further integrated in a parameter estimation procedure, however, in this work we show only a first rudimentary attempt to handle this possibility. An interesting and computationally efficient alternative is the use of the MAER as objective function, i.e. the combination of objective functions defined

in the time (MAE) and in the frequency domain (R), respectively. We show that for our case study overparameterization is not inherently affecting the problem, but it is caused by the approach chosen for the sensitivity analysis and parameter calibration. The proposed approach reduces the issue of overparameterization because also weak processes (and parameters) which are overlaid by stronger effects in the time series can be identified by filtering the signal with the wavelet transform. Since the wavelet-based sensitivity analysis isolates processes occurring at different temporal scales, a temporal scale-based model calibration may lead to more robust results in the sense that they may show the same error but a more physically correct behavior: parameter optimization could be done with a prioritization towards the most relevant scales. By doing so one should overcome equifinal local optima representing unphysical model states. The sensitivity analysis performed in the wavelet domain in this study has not shown a significant effect on the convergence of the sensitivity indices. Future studies should also consider the possibility of performing not only a sensitivity analysis at multiple levels, but also take advantage of the possibility of performing the sensitivity analysis for different time windows, hence combining multilevel and time-dependent sensitivity analysis methods.

Supplementary Information The online version contains supplementary material available at https://doi.org/10.1007/s00477-023-02654-3.

Acknowledgements We acknowledge two anonymous reviewers for their constructive comments. Financial support for G. Chiogna, G. Marcolini, and B. Wohlmuth was provided by DFG in the Project Hydromix (CH 981/4-1 and WO 671/16-1). M. Engel receives funding from the German Federal Ministry of Education and Research on the basis of a decision by the German Bundestag under funding reference 02WGW1662E (KIMoDIs).Open Access funding enabled and organized by Projekt DEAL.

Author contributions GC and GM wrote the main manuscript text and performed the simulations. All authors reviewed the manuscript and participated to the discussion of the results and the development of the methodology.

Funding Open Access funding enabled and organized by Projekt DEAL.

Declarations

Conflict of interest The authors declare no competing interests.

References

Bakker M (2019) Analytic solutions for tidal propagation in multilayer coastal aquifers. Water Resour Res 55:3452–3464. https://doi.org/10.1029/2019WR024757

Basilio Hazas M, Marcolini G, Castagna M, Galli M, Singh T, Wohlmuth B, Chiogna G (2022) Drought conditions enhance groundwater table fluctuations caused by hydropower plant management. Water Resour Res 58:e2022WR032712

Beven K (2006) A manifesto for the equifinality thesis. J Hydrol 320:18–36

Bittner D, Parente MT, Mattis S, Wohlmuth B, Chiogna G (2020) Identifying relevant hydrological and catchment properties in active subspaces: an inference study of a lumped karst aquifer model. Adv Water Resour 135:103472

Bittner D, Engel M, Wohlmuth B, Labat D, Chiogna G (2021) Temporal scale-dependent sensitivity analysis for hydrological model parameters using the discrete wavelet transform and active subspaces. Water Resour Res 57:e2020WR028511

Bittner D, Richieri B, Chiogna G (2021b) Unraveling the time-dependent relevance of input model uncertainties for a lumped hydrologic model of a pre-alpine karst system. Hydrogeol J. https://doi.org/10.1007/s10040-021-02377-1

Borgonovo E, Lu X, Plischke E, Rakovec O, Hill MC (2017) Making the most out of a hydrological model data set: sensitivity analyses to open the model black-box. Water Resour Res 53:7933–7950. https://doi.org/10.1002/2017WR020767

Bruder A, Tonolla D, Schweizer SP, Vollenweider S, Langhans SD, Wüest A (2016) A conceptual framework for hydropeaking mitigation. Sci Total Environ 568:1204–1212

Brunetti G, Šim\uunek, J., Turco, M., Piro, P., (2018) On the use of global sensitivity analysis for the numerical analysis of permeable pavements. Urban Water J 15:269–275

Chiogna G, Marcolini G, Liu W, Ciria TP, Tuo Y (2018) Coupling hydrological modeling and support vector regression to model hydropeaking in alpine catchments. Sci Total Environ 633:220–229

Ciria TP, Labat D, Chiogna G (2019) Detection and interpretation of recent and historical streamflow alterations caused by river damming and hydropower production in the Adige and Inn river basins using continuous, discrete and multiresolution wavelet analysis. J Hydrol 578:124021

Ciriello V, Di Federico V, Riva M, Cadini F, De Sanctis J, Zio E, Guadagnini A (2013) Polynomial chaos expansion for global sensitivity analysis applied to a model of radionuclide migration in a randomly heterogeneous aquifer. Stoch Env Res Risk Assess 27:945–954

Dell'Oca A, Riva M, Guadagnini A (2017) Moment-based metrics for global sensitivity analysis of hydrological systems. Hydrol Earth Syst Sci 21:6219–6234

Duran L, Massei N, Lecoq N, Fournier M, Labat D (2020) Analyzing multi-scale hydrodynamic processes in karst with a coupled conceptual modeling and signal decomposition approach. J Hydrol 583:124625

Ferencz SB, Cardenas MB, Neilson BT (2019) Analysis of the effects of dam release properties and ambient groundwater flow on surface water-groundwater exchange over a 100-km-long reach. Water Resour Res 55:8526–8546

Guse B, Kiesel J, Pfannerstill M, Fohrer N (2020) Assessing parameter identifiability for multiple performance criteria to constrain model parameters. Hydrol Sci J 65:1158–1172

Hauer C, Siviglia A, Zolezzi G (2017) Hydropeaking in regulated rivers: from process understanding to design of mitigation measures. Sci Total Environ 579:22–26

Heil CE, Walnut DF (1989) Continuous and discrete wavelet transforms. SIAM Rev 31:628–666

Herman JD, Reed PM, Wagener T (2013) Time-varying sensitivity analysis clarifies the effects of watershed model formulation on model behavior. Water Resour Res 49:1400–1414

Hucks Sawyer A, Bayani Cardenas M, Bomar A, Mackey M (2009) Impact of dam operations on hyporheic exchange in the riparian zone of a regulated river. Hydrol Process Int J 23:2129–2137

Kirchner JW (2006) Getting the right answers for the right reasons: Linking measurements, analyses, and models to advance the science of hydrology. Water Resour Res. https://doi.org/10.1029/2005WR004362

Labat, D., 2010. Wavelet analyses in hydrology. In: Advances in data-based approaches for hydrologic modeling and forecasting. World Scientific, (pp 371–410)

Meles MB, Goodrich DC, Gupta HV, Shea Burns I, Unkrich CL, Razavi S, Guertin DP (2021) Multi-criteria, time dependent sensitivity analysis of an event-oriented, physically-based, distributed sediment and runoff model. J Hydrol 598:126268. https://doi.org/10.1016/j.jhydrol.2021.126268

Merchán-Rivera P, Geist A, Disse M, Huang J, Chiogna G (2022) A Bayesian framework to assess and create risk maps of groundwater flooding. J Hydrol 610:127797

Pianosi F, Beven K, Freer J, Hall JW, Rougier J, Stephenson DB, Wagener T (2016) Sensitivity analysis of environmental models: a systematic review with practical workflow. Environ Model Softw 79:214–232

Rathinasamy M, Khosa R, Adamowski J, Ch S, Partheepan G, Anand J, Narsimlu B (2014) Wavelet-based multiscale performance analysis: an approach to assess and improve hydrological models. Water Resour Res 50:9721–9737

Reusser DE, Buytaert W, Zehe E (2011) Temporal dynamics of model parameter sensitivity for computationally expensive models with the Fourier amplitude sensitivity test. Water Resour Res. https://doi.org/10.1029/2010WR009946

Rossi A, Massei N, Laignel B, Sebag D, Copard Y (2009) The response of the Mississippi river to climate fluctuations and reservoir construction as indicated by wavelet analysis of streamflow and suspended-sediment load, 1950–1975. J Hydrol 377:237–244

Saltelli A, Annoni P, Azzini I, Campolongo F, Ratto M, Tarantola S (2010) Variance based sensitivity analysis of model output. Design and estimator for the total sensitivity index. Comput Phys Commun 181:259–270

Samaniego L, Kumar R, Attinger S (2010) Multiscale parameter regionalization of a grid-based hydrologic model at the mesoscale. Water Resour Res. https://doi.org/10.1029/2008WR007327

Sarrazin F, Pianosi F, Wagener T (2016) Global sensitivity analysis of environmental models: convergence and validation. Environ Model Softw 79:135–152

Schaefli B, Zehe E (2009) Hydrological model performance and parameter estimation in the wavelet-domain. Hydrol Earth Syst Sci 13:1921–1936

Schöniger A, Wöhling T, Samaniego L, Nowak W (2014) Model selection on solid ground: rigorous comparison of nine ways to evaluate Bayesian model evidence. Water Resour Res 50:9484–9513. https://doi.org/10.1002/2014WR016062

Seibert J, Staudinger M, van Meerveld HJ (2019) Validation and overparameterization—Experiences from hydrological modeling. Computer simulation validation: fundamental concepts, methodological frameworks, and philosophical perspectives 811–834.

Serrano SE, Workman SR (1998) Modeling transient stream/aquifer interaction with the non-linear Boussinesq equation and its analytical solution. J Hydrol 206:245–255

Siena M, Riva M (2020) Impact of geostatistical reconstruction approaches on model calibration for flow in highly heterogeneous aquifers. Stoch Env Res Risk Assess 34:1591–1606

Singh SK (2004) Aquifer response to sinusoidal or arbitrary stage of semipervious stream. J Hydraul Eng 130:1108–1118

Slooten LJ, Carrera J, Castro E, Fernandez-Garcia D (2010) A sensitivity analysis of tide-induced head fluctuations in coastal aquifers. J Hydrol 393:370–380. https://doi.org/10.1016/j.jhydrol.2010.08.032

Smith, R.C., 2013. Uncertainty quantification: theory, implementation, and applications. Siam.

Song X, Zhang J, Zhan C, Xuan Y, Ye M, Xu C (2015) Global sensitivity analysis in hydrological modeling: review of concepts, methods, theoretical framework, and applications. J Hydrol 523:739–757

Torrence C, Compo GP (1998) A practical guide to wavelet analysis. Bull Am Meteor Soc 79:61–78

Wagener T, Pianosi F (2019) What has Global sensitivity analysis ever done for us? A systematic review to support scientific advancement and to inform policy-making in earth system modelling. Earth Sci Rev 194:1–18

Wang H, Chen Y, Li W (2014) Hydrological extreme variability in the headwater of Tarim River: links with atmospheric teleconnection and regional climate. Stoch Env Res Risk Assess 28:443–453

Xiao S, Lu Z, Wang P (2018) Multivariate global sensitivity analysis for dynamic models based on wavelet analysis. Reliab Eng Syst Saf 170:20–30

Yang J, McMillan H, Zammit C (2017) Modeling surface water–groundwater interaction in New Zealand: model development and application. Hydrol Process 31:925–934

Ziliotto F, Basilio Hazas M, Rolle M, Chiogna G (2021) Mixing enhancement mechanisms in aquifers affected by hydropeaking: insights from flow-through laboratory experiments. Geophys Res Lett 48:e2021GL095336

Zolezzi G, Bellin A, Bruno MC, Maiolini B, Siviglia A (2009) Assessing hydrological alterations at multiple temporal scales: Adige River Italy. Water Resour Res. https://doi.org/10.1029/2008WR007266